Supporting Information

A Highly Selective and Rapid Solvatochromic Material for Amide Solvents Detections

Xinyang Zhang,[a] Yunna Zhao,[a] Yi Wei,[a] Lei Qiu,[a] Wei Wang,[a] Zhennan Wang,[a] Hang Yang,[a] Keqiang Chen,[a] Maxim S. Molokeev [cde] and Guogang Li*[ab]

a. Faculty of Materials Science and Chemistry, China University of Geosciences, 388 Lumo Road, Wuhan, Hubei 430074, P. R. China. E-mail: ggli@cug.edu.cn

b. Zhejiang Institute, China University of Geosciences, Hangzhou, 311305, China

c. Laboratory of Crystal Physics, Kirensky Institute of Physics, Federal Research Center KSC SB RAS, Krasnoyarsk 660036, Russia

d. Siberian Federal University, Krasnoyarsk 660041, Russia

e. Department of Physics, Far Eastern State Transport University, Khabarovsk 680021, Russia

† Electronic Supplementary Information (ESI) available: Experimental section and characterization details, additional SEM images, photoluminescence emission spectra, PL decay curves, XRD patterns, UV/Visible absorption spectrum, XPS spectra, ICP-MS results, Rietveld refinement results and additional pictures. See DOI: 10.1039/x0xx00000x

Table of Contents

1. Experimental Procedures 2
2. Results and Discussion 3
3. References 21

1. Experimental Procedures

1) **Materials:** All chemicals were commercially purchased and used without further purification. CuBr (99%), $ZnBr_2$ (99.9%), $MnBr_2$ (99%), CsCl (99.99%), $ZnCl_2$ (99.95%) were purchased from Shanghai Macklin Biochemical Co., Ltd. CsBr (99.999%), CuCl (≥ 99.95%), Hydrobromic acid (ACS 48%), H_3PO_2 (A.R. 50 wt% in water), N,N-dimethylacetamide (DMA) (GC, ≥ 99.8%), N-methyl-pyrrolidone (NMP) (A.R.), N,N-Diethylformamide (DEF) (99%), Diethanolamine (99%), n-octanoic acid (C.P.) were purchased from Shanghai Aladdin Biochemical Technology Co., Ltd. Hydrochloric acid (A.R.), ethanol (A.R. 95%), N, N-dimethylformamide (DMF) (A.R.), Methanol (A.R.), glycol (A.R.), isopropanol (A.R.), methylamine (C.P.), formic acid (A.R. 98%), acetic acid (A.R.), n-caproic acid (C.P.), methyl acetate (A.R.), Ethyl acetate (A.R.), n-hexane (A.R.), n-octane (C.P.), n-propylamine (≥99.5%), toluene (A.R.), formalin (A.R.), ether (A.R.), acetone (A.R.), acetonitrile (A.R.) were purchased from Sinopharm Chemical Reagent Co., Ltd. Cyclohexane was purchased from Tianjin Baishi Chemical Co., Ltd. Diethylene glycol (98%) was purchased from Tianjin Guangfu Fine Chemical Research Institute. Tertiary-butyl alcohol (A.R.), tetrahydrofuran (A.R.), acrylic acid (A.R.) were purchased from Tianjin Damao Chemical Co., Ltd. Screen printing table, flat head scraper and other tools were purchased, and the printing template is customized by the factory.
2) **Preparation of pristine and Cu-doped Cs_2ZnBr_4:** Cs_2ZnBr_4 was prepared by mixing 4 mmol of CsBr with 2 mmol of $ZnBr_2$ in 10 mL of HBr and 1 mL of H_3PO_2 (H_3PO_2 acts as a reducing agent to prevent Cu^+ oxidation) aqueous solution. The solution was heated and stirred at 100 °C for 1 h, turning to a colorless transparent solution. Then, the stirring was stopped, and the white transparent flake-like crystals were obtained by slowly cooling the saturated solution to room temperature. For the Cu-doped Cs_2ZnBr_4 single crystal, the same method was used. The amount of CsBr, $ZnBr_2$, HBr and H_3PO_2 aqueous solution remained unchanged, and different proportions of CuBr were added. For Cu-doped Cs_2ZnCl_4, the same synthesis method was also adopted, but the reactants were replaced with corresponding chlorides and the solvent was replaced with HCl and H_3PO_2 aqueous solution. Mn-doped Cs_2ZnBr_4 was synthesized in the same way through the substitution of CuBr by $MnBr_2$. The crystals were filtered out, then were washed with ethanol and dried overnight in a vacuum at room temperature.
3) **Preparation of test paper:** Cs_2ZnBr_4:Cu powder was applied to the filter paper with a slight wetting condition, then dried to semi-dry and dried naturally to obtain a test paper.
4) **Measurements and characterizations:**
The XRD patterns were recorded on a D8 Focus diffractometer at a scanning rate of 1° min^{-1} in the 2θ range from 5° to 120° with Ni-filtered Cu-Kα (λ = 1.540598 Å). XRD Rietveld profile refinements of the structural models and texture analysis were performed using TOPAS 4.2[1] at room temperature with a Bruker D8 ADVANCE powder diffractometer (Cu-Kα radiation) and linear VANTEC detector. All peaks of the pristine Cs_2ZnBr_4:Cu are indexed by orthorhombic cell (Pnma) with parameters close to Cs_2ZnBr_4[2]. As for DMF-treated sample, all peaks are indexed by orthorhombic cell (Pm-3m) with parameters close to CsBr[3]. Therefore, these structures were taken as starting models for Rietveld refinements. The step size of 2θ was 0.02°, and the counting time was 2 s per step. The morphology, energy-dispersive X-ray spectrum (EDS), and elemental mapping images of the samples were recorded using a field-emission scanning electron microscope (FE-SEM, S-4800, Hitachi, Tokyo, Japan). The diffuse reflectance spectra (DRS) were measured by UV-Visible spectrophotometer (Shimadzu UV-2600). The photoluminescence excitation (PLE), emission (PL) spectra and PL decay curves were measured with a fluorescence spectrometer (Edinburgh Instruments FLS-1000). The power-dependent PL emission was monitored by a power meter of Thorlab PM100D with a standard photodiode power sensor (S120VC). Electron paramagnetic resonance (EPR) measurement was done using a Varian spectrometer (Bruker EMXnano). The selected-area electron diffraction (SAED) and high-resolution transmission electron microscopy (HRTEM) images of Cs_2ZnBr_4:Cu and DMF-treated samples were obtained using a FEI Talos F200X with a field emission gun operating at 200 kV. X-ray photoelectron spectroscopy (XPS) was done with a Thermo Scientific K-ALPHA instrument using monochromatic Al Kα radiation (hv = 1486.7 eV). Inductively coupled plasma-Mass Spectrometry (ICP-MS) was performed on Aglient 7800 ICP-MS. The Fourier transform infrared (FTIR) was done with Thermo Scientific Nicolet iS50.

2. Results and Discussion

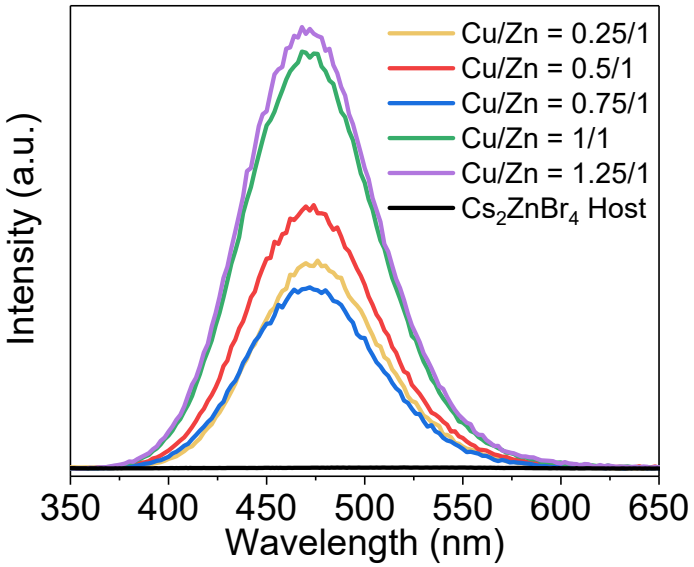

Fig. S1. Photoluminescence emission spectra of Cs_2ZnBr_4 host and Cu doped Cs_2ZnBr_4.

The photoluminescence emission spectra indicate that the introduction of Cu obviously enhances the luminescence of Cs_2ZnBr_4, and the luminescence intensity gradually increases with the increase of Cu/Zn feed ratio.

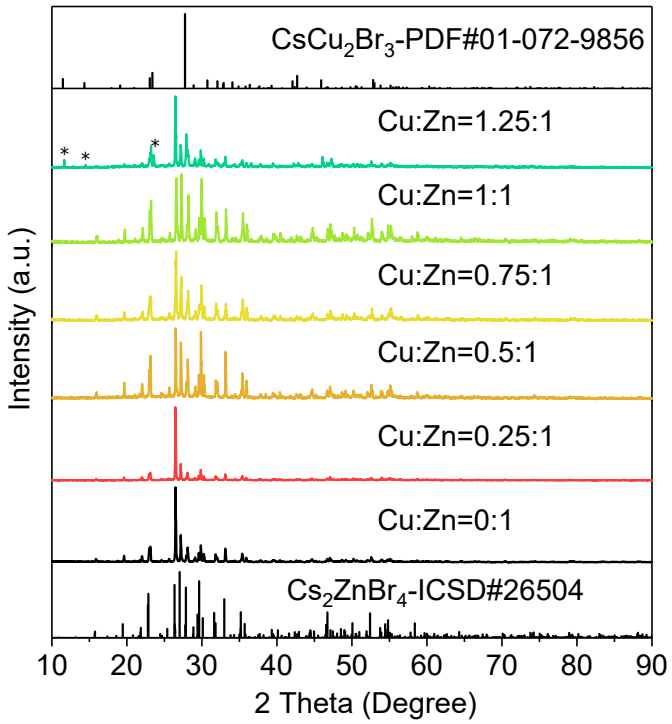

Fig. S2. X-ray diffraction (XRD) patterns of Cs_2ZnBr_4:Cu that are prepared with Cu-to-Zn molar feed ratios of 0:1, 0.25:1, 0.5:1, 0.75:1, 1:1 and 1.25:1. Asterisks denote signals from $CsCu_2Br_3$.

The $CsCu_2Br_3$ impurity phase appears when Cu/Zn radio exceeds 1.25.

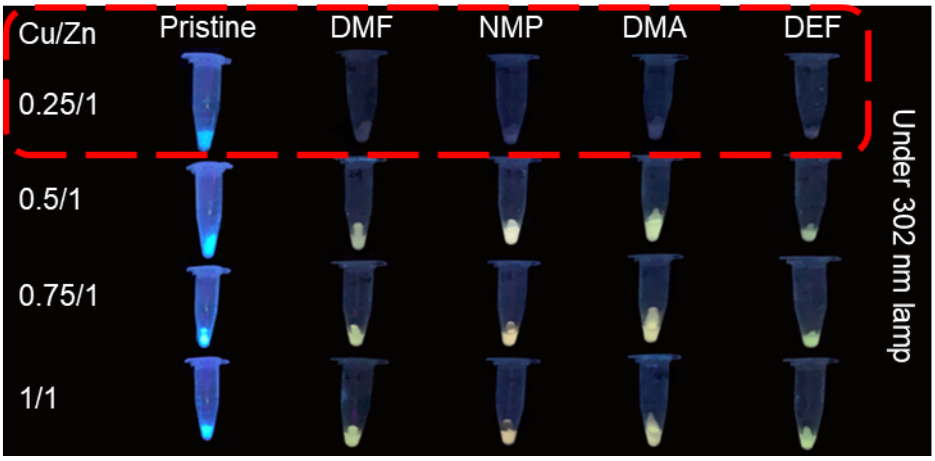

Fig. S3. Photographs of Cs_2ZnBr_4:Cu samples with different Cu/Zn ratios treated with DMF, NMP, DMA, DEF respectively under 302 nm lamp irradiation.

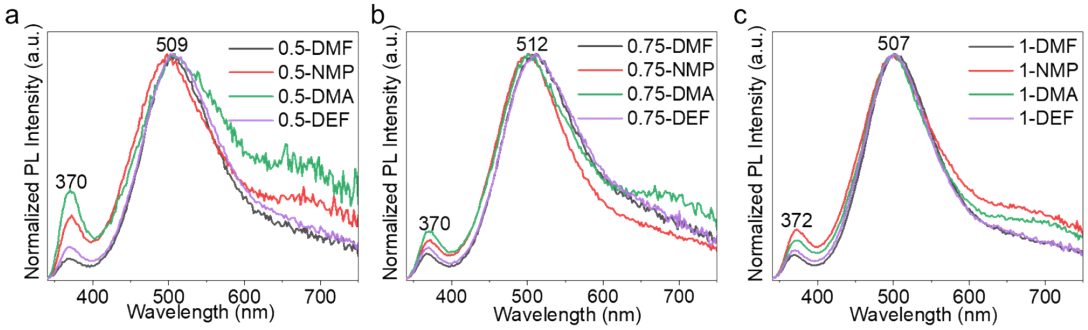

Fig. S4. Photoluminescence emission spectra of (a) Cs_2ZnBr_4:Cu (Zn/Cu = 0.5/1), (b) Cs_2ZnBr_4:Cu (Zn/Cu = 0.75/1), (c) Cs_2ZnBr_4:Cu (Zn/Cu = 1/1) treated with DMF, NMP, DMA, DEF.

For the samples with different Cu/Zn feed ratios (0.5/1; 0.75/1; 1/1), their emission spectra are similar after treating with different amide solvents.

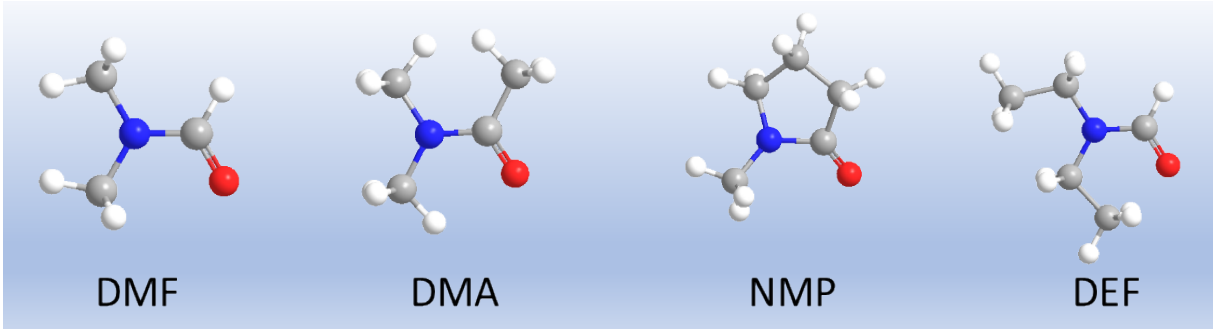

Fig. S5. Chemical structures of the selected amide molecules.

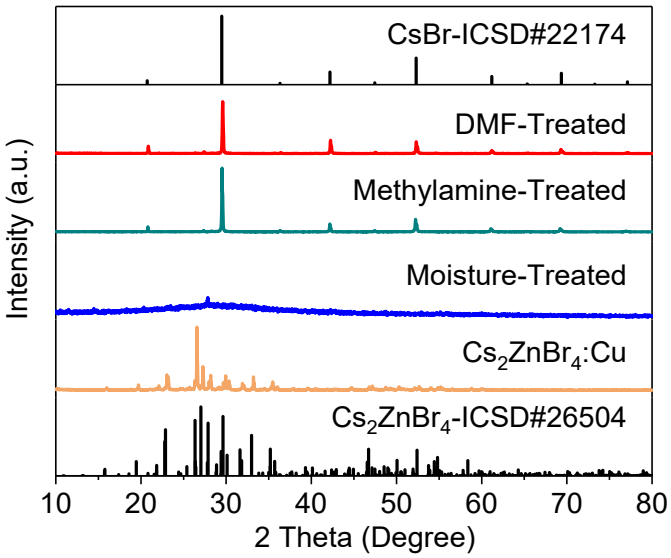

Fig. S6. XRD patterns of the studied samples after dripping with different reagents.

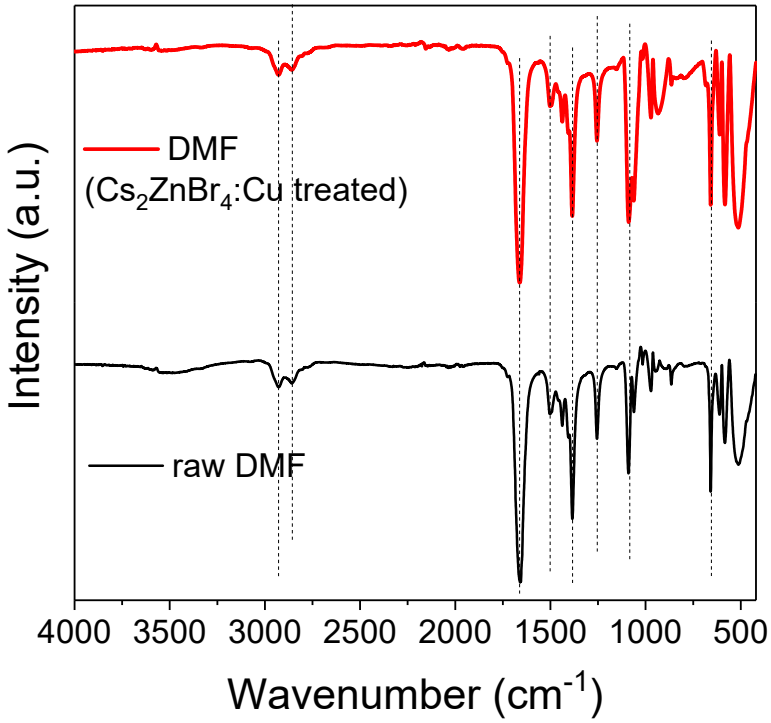

Fig. S7. Fourier transform infrared spectra (FTIR) for pure DMF and Cs_2ZnBr_4:Cu treated DMF

The FTIR peaks of DMF after contacting with Cs_2ZnBr_4:Cu matches well with the pure DMF, and no other peaks appear. This result indicates that the dissolved Cu doesn't form new complexes with DMF.

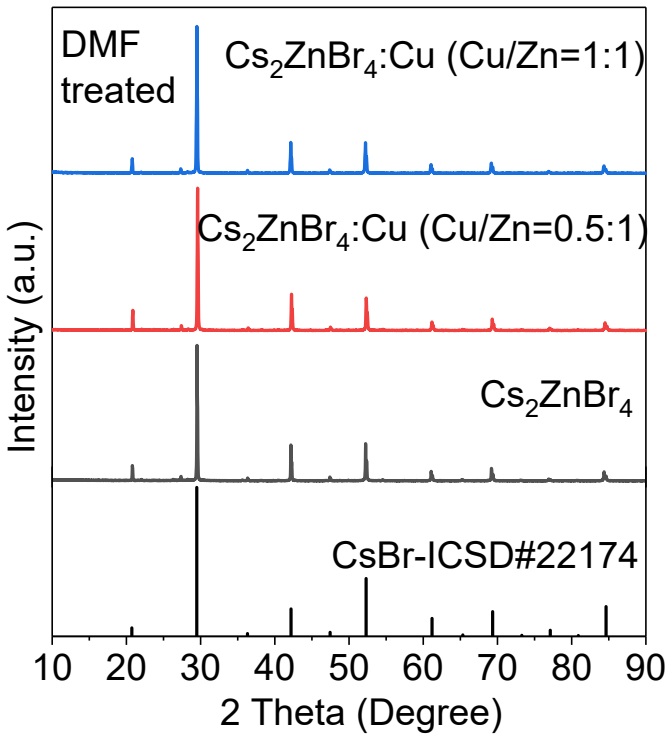

Fig. S8. XRD of DMF-treated Cs_2ZnBr_4:Cu with different Cu/Zn ratios (Cu/Zn=0/1, 0.5/1, 1/1)

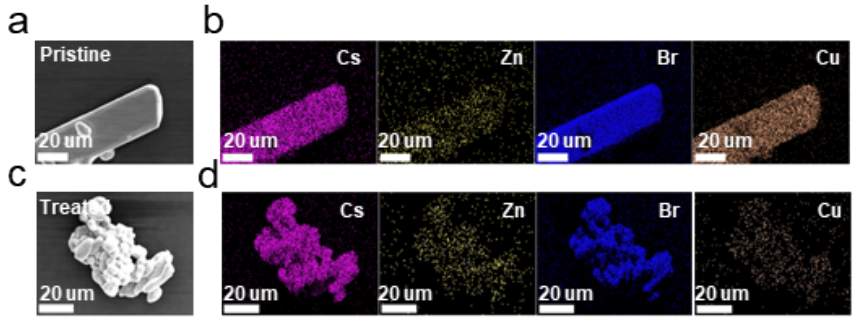

e

Element	Atom% (Pristine)	Atom% (Treated)
Cs	18.00	52.24
Zn	1.60	1.46
Br	45.35	45.28
Cu	35.05	1.02

Fig. S9. (a) SEM images of the Cs_2ZnBr_4:Cu microcrystal particles. (b) Element mapping images of Cs, Zn, Br and Cu for the selected Cs_2ZnBr_4:Cu particle. (c) and (d) corresponding to the DMF-treated sample. (e) Average EDS results (atom %) of the selected particle of the pristine Cs_2ZnBr_4:Cu and DMF-treated sample.

The composition uniformity of samples can be found and Cs, Zn, Br, Cu are homogeneously distributed within the particles. The average atomic ratio of Cs, Zn, Br and Cu is determined by EDS. Due to the same energy of Zn-Kα to Cu-Kα and Zn -Kβ to Cu-Kβ, the atomic ratio of Zn and Cu is not accurate, but generally it can be seen that the atomic ratio of Zn and Cu decreases significantly after DMF treatment, and the remaining components consist chiefly of Cs and Br.

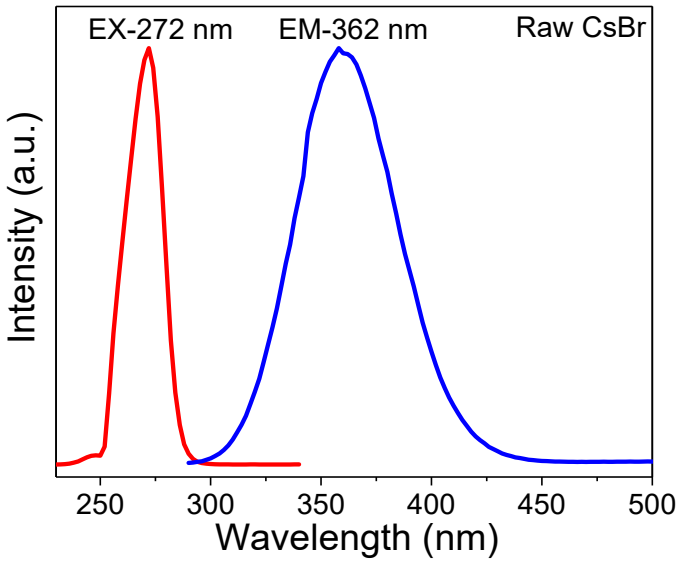

Fig. S10. Photoluminescence excitation and emission spectra of raw CsBr.

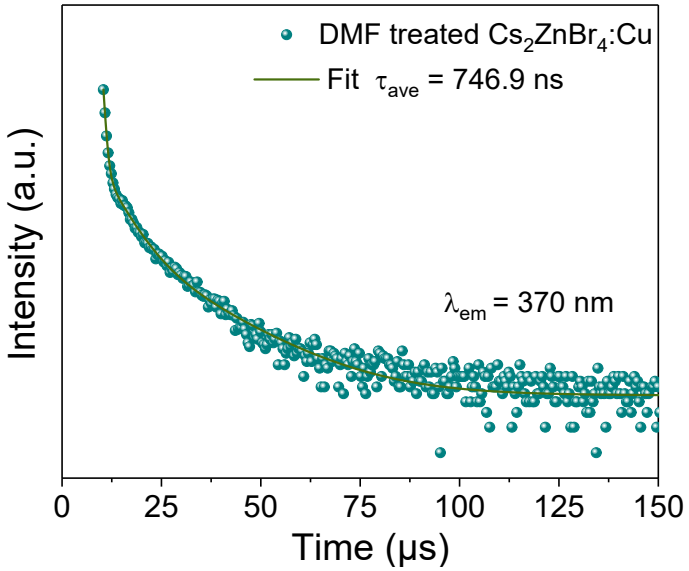

Fig. S11. Photoluminescence (PL) decay curve of the DMF-treated Cs_2ZnBr_4:Cu monitored at 372 nm at room temperature.

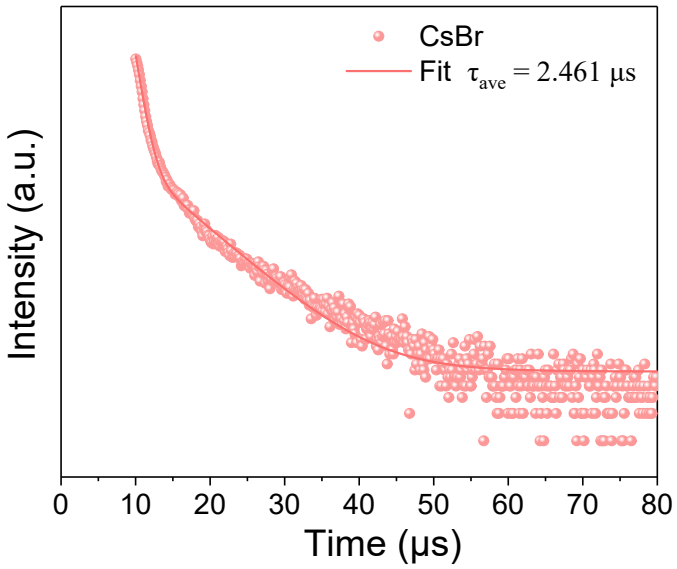

Fig. S12. PL decay curve of the raw CsBr at room temperature.

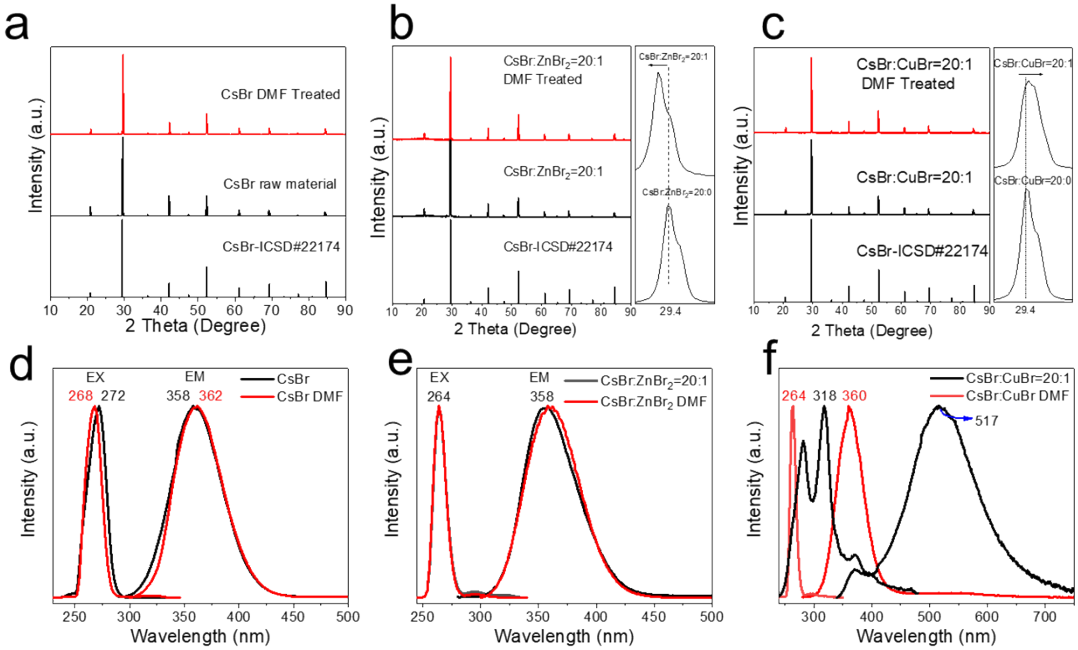

Fig. S13. XRD of (a) raw CsBr and DMF-treated CsBr, (b) CsBr:$ZnBr_2$=20:1 and DMF-treated sample, (c) CsBr:CuBr=20:1 and DMF-treated sample. Excitation and emission spectra of (d) raw CsBr and DMF-treated CsBr, (e) CsBr:$ZnBr_2$=20:1 and DMF-treated sample, (f) CsBr:CuBr=20:1 and DMF-treated sample.

The magnified views in Fig S13b, S13c show the diffraction peak around 29.4 °. Considering the matching of the ion radius, relatively small Cu^+ (R = 0.6 Å, CN = 4) will occupy the Cs^+ (R = 1.74 Å, CN = 8) position when entering the host lattice, and shrinks the lattice, causing the diffraction peak to shift to a large angle. As for CsBr:$ZnBr_2$=20:1 sample, the diffraction peak shifts to a large angle which is an anomaly because the radii of Zn^{2+} (R = 0.6 Å, CN = 4) is also smaller than Cs^+. We speculate that Zn has entered the interstitial site of CsBr rather than occupied the site of Cs^+ which accordingly enlarged the lattice.

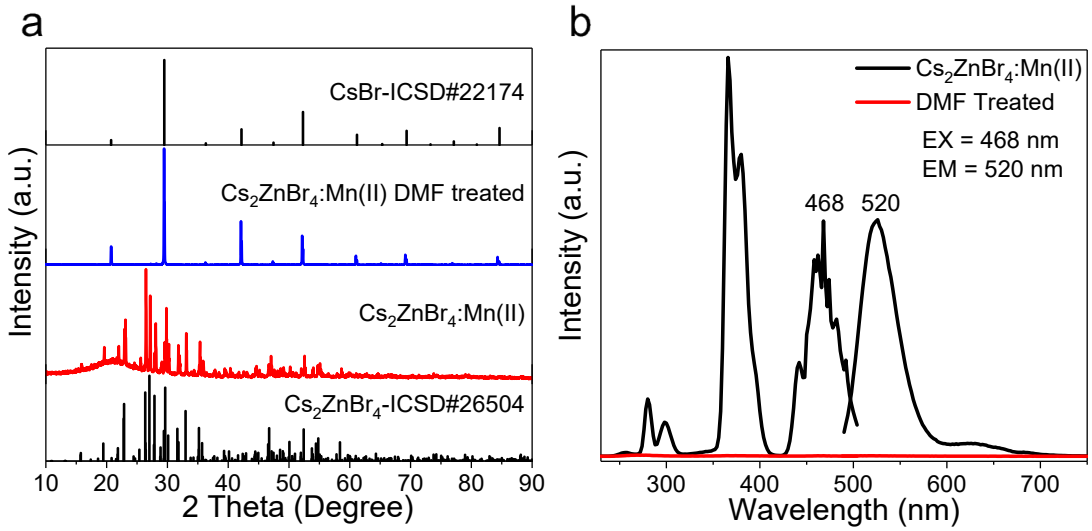

Fig. S14. (a) XRD of Cs_2ZnBr_4:Mn and DMF-treated sample. (b) Excitation and emission spectra of Cs_2ZnBr_4:Mn and DMF-treated sample.

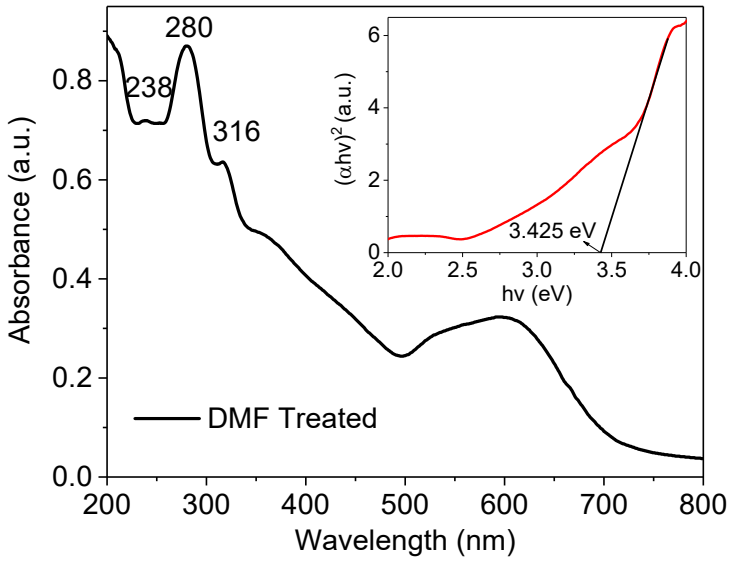

Fig. S15. Ultraviolet (UV)/Visible absorption spectrum of DMF-treated Cs_2ZnBr_4:Cu. The illustration shows the relationship between absorption coefficient and photon energy.

The optical band gap of DMF-treated sample can be obtained from the diffuse reflectance spectrum (DRS). The band gap value can be calculated by the following formulas:

$$(\alpha h\nu)^{\mathrm{n}} = A(h\nu - E_g)$$

$$\alpha = \frac{1-R^2}{2R}$$

where α is the absorption coefficient, hv stands for the incident photon energy, E_g represents the band gap value, and A is a constant. The value of n rests with the type of band gap of the substance: n = 2 for the direct band gap and n = 1/2 for the indirect band gap. After DMF treatment, the phase of sample is linked to CsBr. As CsBr is a direct band gap material[4], so n = 2. R represents the reflectance in the DRS. The optical band gap of DMF-treated sample was calculated to be 3.42 eV.

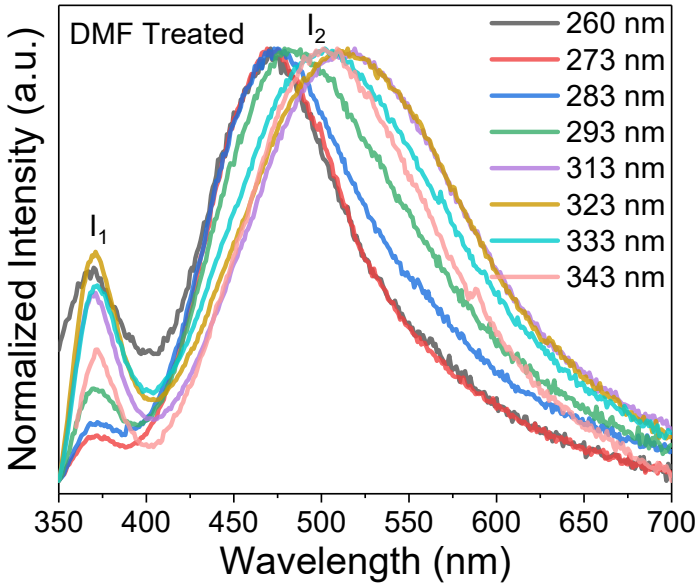

Fig. S16. Emission spectra of DMF-treated sample at diverse excitation wavelengths.

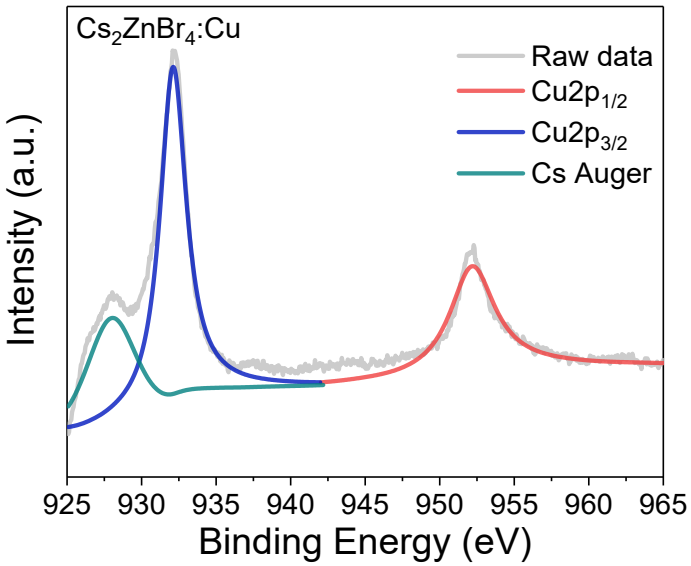

Fig. S17. High-resolution X-ray photoelectron spectroscopic (XPS) analysis of Cu 2p in Cs_2ZnBr_4:Cu.

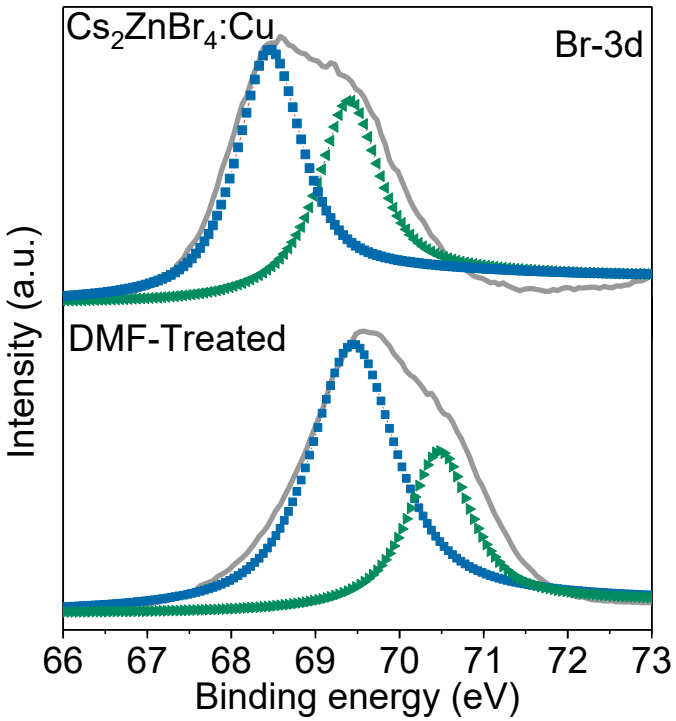

Fig. S18. XPS spectra corresponding to Br 3d in Cs_2ZnBr_4:Cu and DMF-treated sample.

In order to further investigate the distribution of Cu^+ and Cu^{2+}, XPS spectra of Br 3d was conducted. Once Cu^{2+} is introduced into the CsBr, Br will accumulate around Cu^{2+} to maintain charge balance, thus, the distribution of Br can reflect that of Cu^{2+}. The Br 3d peaks can be fitted into two peaks with binding energies of 68.51 and 69.43 eV for pristine Cs_2ZnBr_4:Cu and 69.40 and 70.43 eV for DMF-treated sample, corresponding to the inner and surface Br ions[5], respectively. After treatment, a large shift to large binding energies is observed, and this may result from the immediate variation in coordination environment. As we can see, the intensity ratio between inner and surface Br ions increases after DMF treatment, which can be attributed to the enrichment of the Br content in the inner[6-7]. XPS results indicate that Cu^{2+} is more likely to be doped into the interior of the DMF-treated sample rather than into the surface.

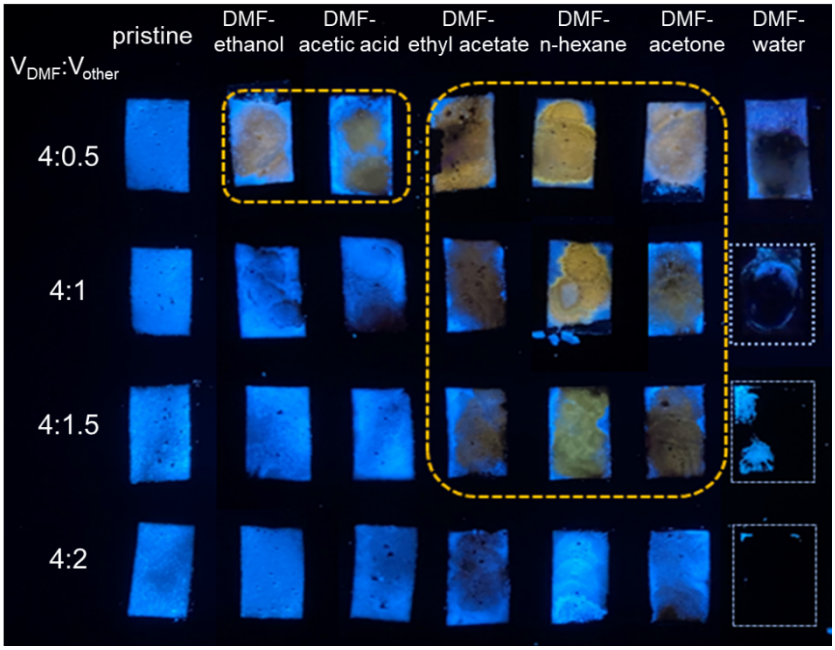

Fig. S19. Photographs of Cs_2ZnBr_4:Cu (Cu/Zn = 0.5/1) treated with different mixed solvents (DMF-ethanol, DMF-acetic acid, DMF-ethyl acetate, DMF-n-hexane, DMF-acetone, DMF-water) with different volume ratios (V_{DMF}:V_{other} = 4:0.5, 4:1, 4:1.5, 4:2) under 302 nm lamp irradiation.

As we can see, in the case of the DMF contained mixed solvents, this material can also exhibits good sensor function. For DMF-ethanol and DMF-acetic acid mixed solvents, when the DMF volume concentration is smaller than 89%, the solvatochromic effect is immeasurable. As for DMF-ethyl acetate, DMF-n-hexane, DMF-acetone, the measurable volume concentration range of DMF is 73%~100%. Besides, if DMF is mixed with water, the luminescence will be quenched.

Table S1. The optical response of Cs_2ZnBr_4:Cu to 30 species of common solvents.

Solvent	Optical phenomenon
Methanol	-
Ethanol	-
Glycol	-
diethylene glycol	-
Isopropanol	-
tertiary-butyl alcohol	-
formic acid	-
acetic acid	-
n-caproic acid	-
n-octanoic acid	-
acrylic acid	-
methyl acetate	-
ethyl acetate	-
n-hexane	-
n-octane	-
Cyclohexane	-
Tetrahydrofuran	-
Acetone	-
Acetonitrile	-
methylamine	luminescence quenching
n-propylamine	luminescence quenching
Diethanolamine	luminescence quenching
Toluene	-
formaldehyde aqueous solution	luminescence quenching
ether	-
distilled water	luminescence quenching
DMF	from blue to yellowish
NMP	from blue to gamboge
DMA	from blue to yellow
DEF	from blue to yellowish

[-] No change.

Table S2. ICP-MS result of Cs_2ZnBr_4:Cu (Zn/Cu=1/0.5) and DMF -treated sample.

Sample	Cs_2ZnBr_4:Cu	DMF-treated Cs_2ZnBr_4:Cu
Cs^+ concentration (μg/kg)	387307692	673579802
Cu^+ concentration (μg/kg)	64397703	1058124
Zn^{2+} concentration (μg/kg)	87328793	22721821
Cu-to-Cs molar ratio	34.77%	0.33%
Zn-to-Cs molar ratio	45.81%	6.85%

Table S3. Main parameters of processing and refinement of the Cs_2ZnBr_4:Cu sample.

Compound	Cs_2ZnBr_4:Cu
Sp. Gr.	*Pnma*
a (Å)	10.2037(3)
b (Å)	7.7443(2)
c (Å)	13.5393(4)
V (Å^3)	1069.88(5)
Z	4
2ϑ-interval, º	7-120
R_{wp},%	7.56
R_p,%	5.63
χ^2	2.04
R_B,%	3.09

Table S4. Main parameters of processing and refinement of the DMF-treated samples.

Compound	CsBr
Sp. Gr.	*Pm*-3*m*
a (Å)	4.298359(62)
V (Å^3)	79.4160(34)
Z	1
2ϑ-interval, º	5-120
R_{wp},%	5.34
R_p,%	8.1
χ^2	54.8
R_B,%	1.84

Table S5. Fractional atomic coordinates and isotropic displacement parameters (Å²) of Cs_2ZnBr_4:Cu

Atom	*x*	*y*	*z*	B_{iso}	*Occ.*
Cs1	0.6350(3)	0.25	0.3957(2)	5.6(3)	1
Cs2	0.4774(3)	0.25	0.8292(2)	3.9(3)	1
Zn	0.2332(5)	0.25	0.4204(5)	3.5(3)	1
Br1	0.0060(4)	0.25	0.4011(3)	4.7(3)	1
Br2	0.3114(5)	0.25	0.5876(3)	4.8(3)	1
Br3	0.3274(4)	0	0.3456(3)	4.9(3)	1

Table S6. Fractional atomic coordinates and isotropic displacement parameters (Å²) of DMF-treated samples

Atom	*x*	*y*	*z*	B_{iso}	*Occ.*
Cs	0	0	0	1.17(14)	1
Br	0.5	0.5	0.5	1.32(13)	1

Table S7. Main bond lengths (Å) of Cs_2ZnBr_4:Cu.

Zn—Br1	2.3330(66)	Zn—Br2	2.4003(78)
Zn—Br3	2.3870(43)		

Table S8. Main bond lengths (Å) of DMF-treated samples.

Cs—Br	3.72250(10)

References

1 Bruker AXS TOPAS V4: General profile and structure analysis software for powder diffraction data. – User's Manual. Bruker AXS, Karlsruhe, Germany. 2008.

2 B. Morosin, E. C. Lingafelter, *Acta Cryst.,* 1959, **12**, 744.

3 D. L. Fancher, G. R. Barsch, *J. Phys. Chem. Solids,* 1969, **30**, 2503-2516.

4 S. Wei, C. Zhu, Q. Li, Y. Zhou and Q. Li, Y. Ma, *Phys. Chem. Chem. Phys.,* 2014, **16**, 17924-17929.

5 F. Li, Y. Liu, H. Wang, Q. Zhan, Q. Liu and Z. Xia, *Chem. Mater.,* 2018, **30**, 8546-8554.

6 F. Zhang, H. Zhong and C. Chen, *ACS Nano,* 2015, **9**, 4533-4542.

7 J. Zhou, M. Li, L. Ning, R. Zhang, M. S. Molokeev, J. Zhao, S. Yang, K. Han and Z. Xia, *J. Phys. Chem. Lett.,* 2019, **10**, 1337-1341.